Available online at www.sciencedirect.com
ScienceDirect
Energy Procedia 50 (2014) 761 – 772
Energy Procedia

The International Conference on Technologies and Materials for Renewable Energy, Environment and Sustainability, TMREES14

CFD based analysis of heat transfer enhancement in solar air heater provided with transverse rectangular ribs

A.Boulemtafes-Boukadoum[a]*, A.Benzaoui[b]

[a]*Centre de Développement des Energies Renouvelables, CDER, Algiers, 16340, Algeria*
[b]*Laboratoire Thermodynamique et Systemes Energetiques, Faculté de Physique, USTHB, Algiers, 16000, Algeria*

Abstract

A numerical analysis of convective heat transfer enhancement in solar air heaters with artificially roughened absorber is presented in this paper. CFD numerical simulations were carried out to analyze the flow and heat transfer in the air duct of a solar air heater provided with transverse rectangular ribs. The air flows in forced convection and the absorber is heated with uniform flux. Since the flow is turbulent, we used the RANS formulation to model the flow. We solved continuity, momentum and energy equations in turbulent mode using four closure models: k-ε RNG, k-ε RZ, k-ω Standard, k-ω SST. A two-dimensional non uniform grid was generated according to used geometry, with local refining near the wall, in order to critically examine the flow and heat transfer in the inter-rib region. The effect of major parameters (Reynolds number, Nusselt number, friction factor, global thermohydraulic performance parameter…etc) is examined and discussed. The results obtained are concordant to those found in the literature and shows clearly the heat transfer enhancement without big penalty of friction losses.

Selection and peer-review under responsibility of the Euro-Mediterranean Institute for Sustainable Development (EUMISD)
Keywords: solar air heater; artificial roughness; rectangular ribs, CFD analysis; turbulence; heat transfer enhancement.

1. Introduction

Energy efficiency and energy savings are one of the major scientists concerns in the last decade because of the increase in energy global demand and consumption as result of economic development and population growth. The

* Corresponding author. Tel.: +213-21-901503; fax: +213-21-901560.
E-mail address: a.boulemtafes@cder.dz

Selection and peer-review under responsibility of the Euro-Mediterranean Institute for Sustainable Development (EUMISD)
doi:10.1016/j.egypro.2014.06.094

Nomenclature

ρ	air density
D_h	hydraulic diameter
h	convective heat transfer
h	duct height
L	duct length
u^+	adimensional velocity
u_m	mean flow velocity
ΔP	the pressure drop between the inlet and the outlet of the duct
δ_t	sublayer thickness
λ	thermal air conductivity
ν	fluid kinematic viscosity
τ_w	wall shear stress

conversion, utilization and recovery of energy, invariably involve a heat exchange process, which makes it imperative to improve the thermal performance of heat exchangers. Solar collectors, as particular type of heat exchangers, are the basic elements in all solar radiation conversion systems into heat at low temperatures. They are adapted to applications that need heat temperature between 30° and 70°C. They are used in many applications, such as local space heating, water heating and solar drying of agricultural produces.

Solar air heaters (SAH) are used to convert solar radiation into heat using flowing air. They are composed of a glazing, an absorber, and an insulated box. SAH are generally classified into three types according to air passes:

- type I with air flowing between the absorber plate and the cover glazing;
- type II with air flowing between the absorber plate and the back panel;
- and type III with two air channels above and below the absorber plate.

However, SAH's thermal efficiency is actually poor because of the bad heat transfer between the flowing air and the heated absorber [1]. This is due to the low thermophysical properties of the air in part, and to the viscous sublayer that appears in the vicinity of the absorber and which is resistant to the heat transfer in the other part.

In order to make solar air heaters more efficient, their thermal efficiency needs to be improved. Many techniques based on both active and passive methods have been proposed to enhance heat transfer in these applications [2]. Among these methods one can find systems involving vortex generators such as ribs and baffles. Disturbance promoters increase fluid mixing and interrupt the development of thermal boundary layer, leading to enhancement of heat transfer. The heat transfer enhancement techniques are available to achieve this objective by:

- Increasing the heat-transfer area with the use of extended surfaces, or corrugated ones.
- Enhancing the convective heat transfer coefficient. This may be attained by broking the laminar sub-layer formed in the vicinity of the absorber plate, by introducing artificial roughness on that surface..

In the literature , one can find several studies on solar air heat enhancement techniques. Thus, Varun [3] gave an overview of the geometry of roughness used in heat exchangers and presented a selection of roughness that are adapted to case of solar air collectors . He studied the effect of a large number of parameters such as the shape and size of roughness on the air flow regime. Hans et al. [4] reviewed the roughness element geometries employed by various investigators to improve the thermal performance of solar air heaters. In view of finding optimal roughness pattern, 11 distinct roughness geometries have been compared on the basis of thermohydraulic performance. Recently, Bhushan [5] presented an attempt to classify and examine the geometry of artificial roughness used in duct of solar air collectors . Correlations giving the heat transfer coefficient and the friction coefficient developed by various researchers for solar air heaters provided with artificial roughness were also presented in the paper.

Research studies on artificial roughness using CFD techniques are less numerous. However, one can cite Lee [6], who studied numerically heat transfer and air flow above a horizontal surface provided with two-dimensional roughness using a CFD model. Chaube [7] performed a numerical analysis using Fluent6.1to analyze the effect of nine types of roughness on heat transfer and friction characteristics enhancement. The author reported that in the case of transverse ribs the results obtained from the two-dimensional model are concordant to the experimental results and requires less memory and computation time compared to three-dimensional models. Also, in the transverse ribs, the best performance was obtained with rectangular ones in the range of the studied parameters. Others authors gave their conclusion after performing CFD analysis to study the effect of artificial roughness on heat transfer enhancement in solar air heaters [8,9].

As the air flows over the heated absorber, a viscous sublayer (laminar) appears in the vicinity of the absorber. This sublayer is resistant to the heat transfer between the absorber and the fluid (air). To break it, artificial roughness are provided on the absorber surface. The obstacles or rough elements, whatever their shape, are generating secondary flows or recirculations, which result in two separation zones on both sides of the obstacle. The generated vortices are responsible of the turbulence and thus increase the heat transfer and pressure losses. Secondary fluid circulation promote a better convective heat transfer. However, it is desirable that the turbulence takes place only in the near-wall region, that is to say within the laminar sub-layer, where the heat transfer takes place, to minimize friction losses, Bhatti [10]. This is achieved by keeping the height of the rough element relatively small in comparison to duct dimensions. For remind, the laminar sublayer thickness is given by [10]:

$$\delta_t = 5\frac{\nu}{u_t} \tag{1}$$

for a smooth surface , we have, [4]:

$$u^+ = u\sqrt{\frac{\tau_w}{\rho}} \tag{2}$$

$$y^+ = \frac{y\sqrt{\left(\tau_w/\rho\right)}}{\nu} \tag{3}$$

and we have

$u^+ = y^+$ for the laminar sublayer, $y^+ \leq 5$ (4)

$u^+ = 5\ln y^+ + 3.5$ for the transition layer (buffer), $5 \leq y^+ \leq 30$ (5)

$u^+ = 2.5\ln y^+ + 5.5$ for the turbulent layer, $y^+ > 30$ (6)

There are some basic dimensionless geometrical parameters that are used to characterize roughness [5] :

- Relative roughness pitch (p/e): it is defined as the ratio of distance between two consecutive ribs (p) and height of the rib(e).

- Relative roughness height (e/D): Relative roughness height (e/D) is the ratio of rib height (e) to equivalent diameter of the air duct (D).

- Angle of attack (α): Angle of attack is inclination of rib with direction of air flow in duct.

- Aspect ratio: It is the ratio of duct width to duct height. This factor also plays a very crucial role in investigating thermo-hydraulic performance.

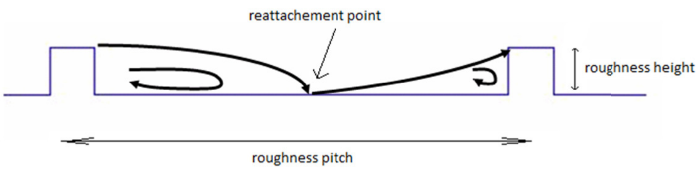

Fig. 1 Flow separation and reattachmentover the rib

The turbulent flow induced by the presence of obstacles is very complex to study, that is why it is very difficult to develop analytical models to predict the fluid motion. One of the first studies on rough surfaces was first provided by Joule [11] to enhance heat transfer coefficients for steam in-tube condensation.we can also cite Nikuradse [12] who made an attempt to approach the velocity and temperature distribution of the flow on a rough surface. Since then many experimental investigations were carried out on in the areas of cooling of gas turbine blades, electronic equipments, nuclear reactors, and compact heat exchangers,...etc. Webb and Eckert [13] conducted experimental study of turbulent air flow in tubes roughened with rectangular repeated ribs and deduced heat transfer and friction factor correlations based on the wall law similarity and heat-momentum transfer analogy. Lewis [14] introduced new efficiency parameter for optimizing thermohydraulic performance of roughened surfaces with respect to smooth surfaces.

Artificial roughness used in solar air heaters are numerous, have different geometries , shapes, sizes , and are produced by various arrangements and orientations. The geometries of various types of roughness reported in the literature , can be divided into two main categories :

- Transverse fixed Roughness (horizontal , inclined , or V-shaped) in continuous or discrete distribution .
- Roughness produced by a traditional manufacturing processes of machining, forming, casting, or welding

In transverse ribs , the friction factor growth is almost twice the increase in heat transfer. The best performance was recorded for ribs with rectangular section [7,15]. For the inclined V-shaped, the friction factor increase is equal to or slightly greater than the increase in the Nusselt number , except for the arc shaped . For rough machined , it is observed that the penalty is approximately triple for the friction factor and the increase in Nusselt number is double, except for the combination of chamfered groove ribs, where the friction factor and heat transfer enhancement are almost equal. However, it was observed that the generation of artificial roughness on the absorber surface, is not easy and may not be economically gainful for large-scale production [16] . Based on this literature review , we chose the study of the influence of transverse roughness of rectangular sections because they have the best performance and are easy to provide by fixation.

1.1. *Thermo-hydraulic performance of solar air heater provided by artificial roughness*

To characterize the heat transfer between the heated absorber and the flowing air in the solar air heater duct , we determined some dimensional numbers that provide required information on the heat transfer quality. These numbers are :

The Nusselt number $$Nu_m = \frac{h_m Dh}{\lambda} \tag{7}$$

The Stanton number $$St = \frac{Nu\,\mathrm{Re}}{\mathrm{Pr}} = \frac{h}{\rho C p u_m} \tag{8}$$

Artificial roughness although it allows an increase in heat transfer also has the undesirable consequence of pressure drop due to friction. Therefore, It is usually necessary to determine the best combination of heat transfer rate increases with the lowest possible pressure losses. For that purpose we used the factor friction expression given by [17]:

$$fr = \frac{\Delta P D_h}{1/2\rho u_m^2 L} \tag{9}$$

in order to analyze overall performance of a solar air heater, thermo-hydraulic performance should be evaluated by considering thermal and hydraulic characteristics of the collector simultaneously. Thermo-hydraulic performance of a solar air heater is given by the following expression introduced by Kumar [8]:

$$E_t = \frac{\left(Nu / Nu_l \right)}{\left(fr / fr_l \right)^{1/3}} \tag{10}$$

2. Solution domain

To study the heat transfer enhancement we choose a rectangular section channel representing the air duct of a solar air heater Type I. The top surface is the glazing and the bottom one is the heated absorber [2] . This surface is provided by rectangular ribs. Air is flowing between the two surfaces in forced convection, Fig.(2).

The first part of the simulation aims to validate our numerical model, so we chose a configuration (1) with the same dimensions that the one studied experimentally by Karwa [15] and numerically by Tanda [18]:

H=40 mm, aspect ratio=7.5, rectangular ribs, e=3.4 mm, w= 5.8 mm , p= 34 mm. The boundary conditions applied to the domain solution :

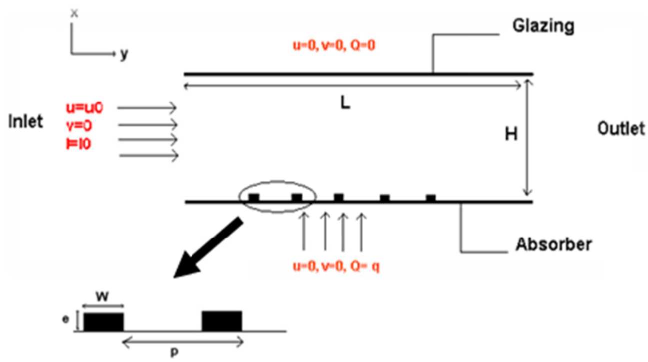

Fig.2 Geometric configuration

<u>At the inlet</u> :T_0=293K, u_0=0.6 to 3.4 m/s, v_0=0, I_0=5%

<u>On the top plate:</u> u=o,v=o, q=0 (adiabatic)

<u>On the bottom plate:</u> u=o, v=o, q= 4 kW/m^2

<u>Oulet :</u> P= P_{atm}

The second configuration (2) is an attempt to approach the solar air heater with optimal operating conditions.We have chosen an air duct with the following geometric parameters: aspect ratio (W/H)=7, P/e = 10, e/D= 0.05. The boundary conditions are:

Inlet: $T=T_0=$ 298 K, $u_0=0.5$ to 4 m/s, $v_0=0$, $I_0=5\%$

On the top plate: u=o,v=o, q=0 (adiabatic)

On the bottom plate : u=o, v=o, q= 600 W/m^2

Outlet : P= P_{atm}

3. Mathematical modelling

Considering the air flow in the channel with heat transfer, the mathematical model applied is composed of the conservation equations of mass, momentum and energy for incompressible flow in two dimensions with the following assumptions:

- The flow is two-dimensional, turbulent and stationary.
- The thermophysical properties of the air are supposed to be constant.
- The thermal conductivity of the walls and ribs is supposed to be constant.

$$\frac{\partial u_i}{\partial x_i} = 0 \tag{11}$$

$$u_j \frac{\partial u_i}{\partial x_j} = -\frac{1}{\rho}\frac{\partial p}{\partial x_i} + \nu\left(\frac{\partial^2 u_i}{\partial x_i^2} + \frac{\partial^2 u_i}{\partial x_j^2}\right) \tag{12}$$

$$u_i \frac{\partial T}{\partial x_j} = a\left(\frac{\partial^2 T}{\partial x_i^2} + \frac{\partial^2 T}{\partial x_j^2}\right) \tag{13}$$

With $a = \dfrac{\lambda}{\rho C_p}$

x_i, cartesian coordinates ($x_i \equiv$ x, y),

u_i, velocity component in x_i direction,

μ dynamic viscosity coefficient.

Since the flow is turbulent, we used Reynolds decomposition to write:

$$u = \overline{u} + u' \tag{14}$$

where $\overline{u}$ is the mean velocity and u' the fluctuation.
In what follows , $\overline{u}$ is simply expressed by u
substituting (14) in (11,12,13), we obtained in tonsorial notations:

$$\frac{\partial}{\partial x_i}(u_i) = 0 \tag{15}$$

$$\rho \frac{\partial}{\partial x_j}\left(u_i u_j\right) = -\frac{\partial p}{\partial x_i} + \frac{\partial}{\partial x_j}\left[\mu\left(\frac{\partial u_i}{\partial x_j} + \frac{\partial u_j}{\partial x_i}\right)\right] - \frac{\partial}{\partial x_j}\overline{\rho u_i' u_j'} \tag{16}$$

These equations are called RANS equations (Reynolds-Averaged Navier Stokes).

$\left(-\overline{\rho u_i' u_j'}\right)$ represents the Reynolds stress tensor and must be properly modeled to close the equations. We used Boussinesq hypothesis which assumes that the Reynolds stress tensor has the same form as a viscous stress tensor, that is to say that the turbulent flow behaves like a fluid viscosity μt which expression depends on the closed model used, [19].

4. Numerical resolution

4.1. *Grid generation*

A two-dimensional non-uniform grid was generated according to the geometry used. In order to examine the flow and heat transfer critically in the inter-rib region, a refining of the grid near the walls was necessary. Several grids were tested in order to check out the solution independence. For all simulations, we verified that y + <5 to solve the equations in the viscous sublayer.

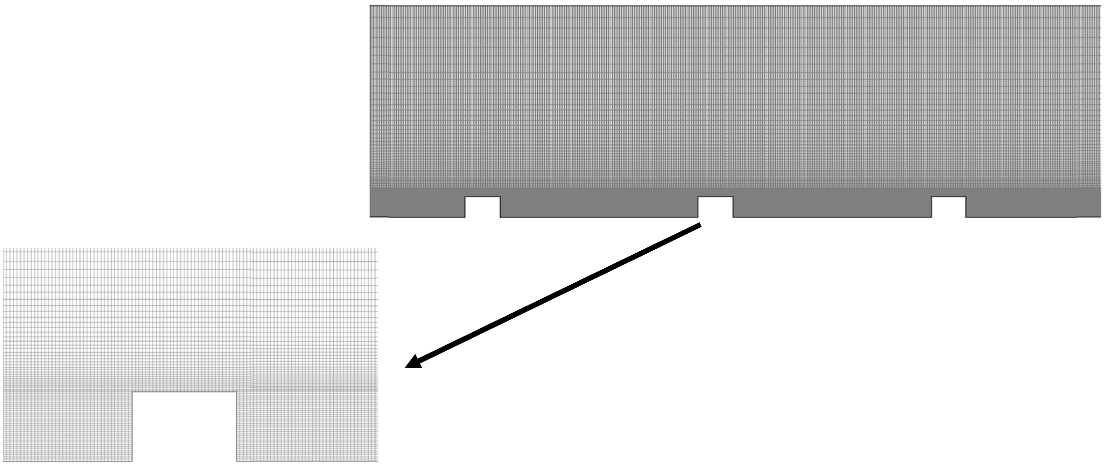

Fig. 3. Numerical grid

4.2. *Numerical resolution*

CFD (Computational Fluid Dynamics) analysis based on Finite Volumes method was used for the resolution of the equations of mass, momentum and energy equations. Second order Upwind scheme was used to discretize the governing equations. The coupling between velocity and the pressure was treated with the SIMPLE algorithm.

The mean inlet velocity of the flow was calculated using Reynolds number. “Velocity inlet” condition has been considered as inlet boundary condition and “Pressure outlet” as outlet boundary condition.

5. Results and discussions

Configuration1

We solved continuity, momentum and energy equations in turbulent mode using four closure models (two-equations models):

- k-ε RNG (Renormalization GroupTheory)
- k-ε RZ (Realizable)
- k-ω Standard
- k-ω SST

For each turbulence model, Reynolds number varied from 3000 to 15000. The same simulation, have been conducted for a smooth duct of same dimensions as roughened one, in order to compare the results and thus highlight the heat transfer enhancement due to artificial roughness.

Stanton number is one of the most important parameters in heat transfer, so we calculated it for different Reynolds numbers. The results obtained using the four turbulent closure models have been compared with Dittus–Boelter empirical correlation for smooth duct given below [17]:

$$Nul = 0.023\,\mathrm{Re}^{0.8}\,\mathrm{Pr}^{0.4} \tag{14}$$

The curve representing the ratio between the Stanton number (St) for the rough duct and smooth one (Stl), versus Reynolds number, is represented in Fig. 4a for different turbulence models used.

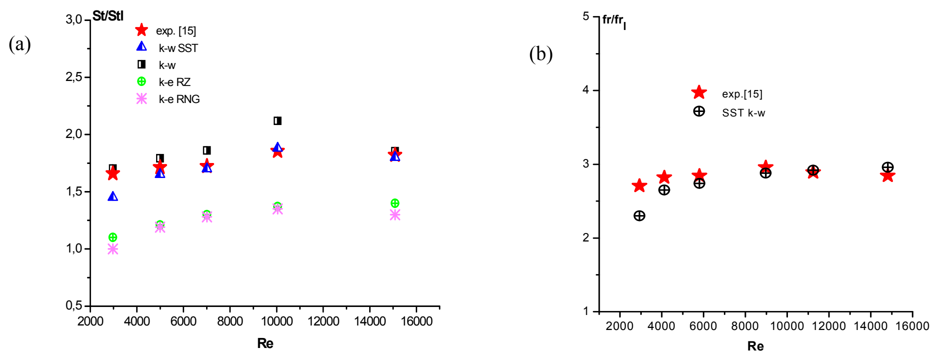

Fig. 4. (a)(St/Stl) versus Re, predicted by the four turbulence models, (b) Friction factor ratio(fr/fr_l) evolution according to Re (SST k- ω)

We noticed that the ratio (St/St_l) increases with the Reynolds number, whatever the turbulence model used. The increase in roughned duct Stanton number is 1.3 to 1.8 times, higher than smooth duct, reaching a peak for Re = 10000. Furthermore this comparison, it is clear that the SST k-ω model gives the best results because its values are close to Karwa's [15] experimental results. Therefore, we will use exclusively this model in further simulations.

To verify that the improved heat transfer induced by artificial roughness is not followed by too much friction loss, we calculated the rough duct friction factor (fr) and smooth duct one (fr_l), for different values of Reynolds number. The latter is calculated by the relation of Blasius, [17]:

$$fr_l = 0.316\,\mathrm{Re}^{-0.25} \tag{15}$$

The ratio (fr/frl) evolution according to Re is shown in Fig. 4b. We observed that our curve shape is similar to Karwa's one [15]. Friction factor values although they are increased by the presence of roughness remain within an acceptable range.

Configuration 2

The goal of this analysis is to understand the heat transfer mechanism between air and heated absorber, mainly in inter-rib area. That is why it is important to analyze the fluid flow characteristics that are responsible of this mechanism. We plotted the velocity vectors distribution (longitudinal component) around the rectangular roughness (Fig. 5), in order to observe more closely the main recirculation zones that appear upstream, above and below the rib. We noticed a first low recirculation zone upstream of the rib that appears when the flow is separated. The second recirculation zone is an over-speed area that appears above the rib, where the fluid velocity increase more than 150 %. Downstream the rib and near the wall, there is a large recirculation zone which is the reattachment area and a small area at the bottom of the roughness which is growing as the Reynolds number increases.

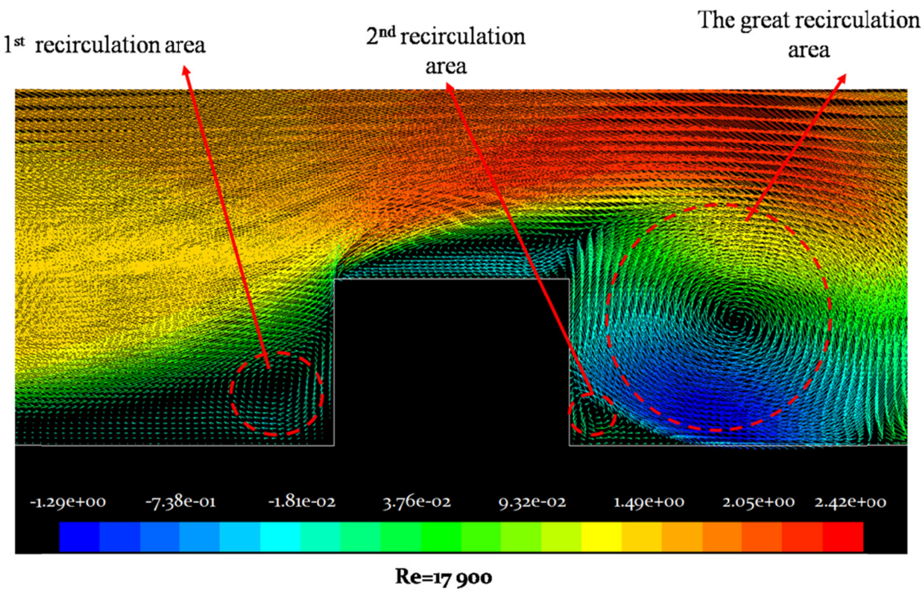

Fig. 5 Velocity vectors distribution (longitudinal component) around the rib

Since the detailed data flow parameters including the separation and reattachment points are very important for analyzing the heat transfer mechanism, we read the reattachment point abscisses of the fluid downstream the rib and the reattachment lengths (Lr) relating. The results obtained are shown in Figure 6. Compared to the results of Chaube [7], they show good agreement with them. We can observe that the lengths decrease gradually after each rib before stabilizing around a constant value which corresponds to fully developed turbulence.

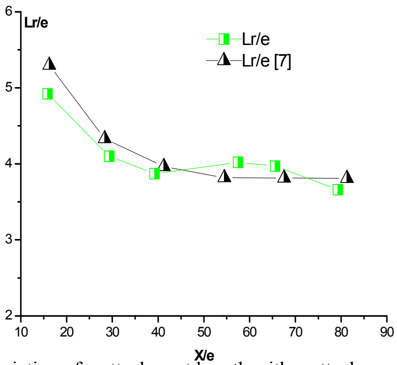

Fig. 6 Variation of reattachment length with reattachment point abscissas

The Figure 7a represents the Nusselt number mean evolution according Reynolds number for rectangular ribs. We observed that Nu increases in an almost linear way with Re. This result was foreseeable because at low Reynolds numbers (laminar flow), Nusselt number for all surface types is barely constant, because of the resistance of the viscous sub-layer to heat transfer. The use of artificial roughness has for effect to break this resistance, and thus increase the heat transfer.

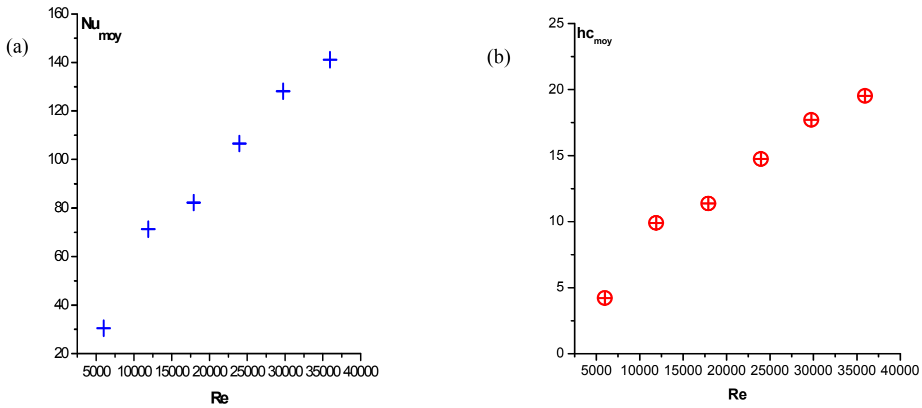

Fig. 7:(a) Nusselt number Vs Re**;** (b)Heat transfer coefficient vs Re

One can note that the heat transfer coefficient (hc) evolution's curve has the same shape as that of Nusselt number (Fig. 7b). Indeed, this one increases regularly with the Reynolds number. However, a high value of Nu_m or hc coefficient doesn't guarantee a good thermal efficiency. Because when the Reynolds number increases, the generated vortex causes also losses of pressure.

For this reason it is significant to estimate the friction factor for the surfaces provided with roughness. This parameter variation has been plotted in Figure 8a. As found in the literature, the friction factor [4] decreases with the increase in the Reynolds number. We can also observe that the values of the factor of friction remain moderate in all the range of Reynolds numbers.

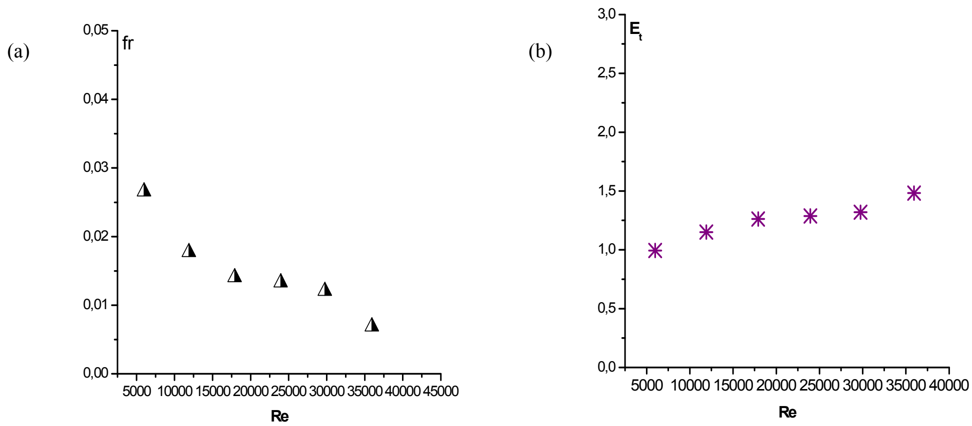

Fig. 8 (a). Effect of Reynolds number on friction factor, (b) Effect of Reynolds Number on global thermohydraulic performance parameter

On Figure8b, we plotted the curve of the global thermohydraulic performance parameter E_T, introduced by Kumar [8]. A good parameter of performance ($E_T > 1$) is recorded in all the range of Reynolds numbers. Moreover, E_T increases appreciably with the increase in the Reynolds number.

The outlet temperature Ts is another significant parameter in solar air heaters because it determines its use (space heating, greenhouse heating or solar drying). We plotted the Ts curve according to Reynolds number on Figure 9. We can note that this one decreases when the speed of the fluid increases. This is a direct consequence of the increase in the factor of friction which decrease the effective heat transfer rate of the wall heated towards the fluid and thus contributes to lower its average temperature at exit.

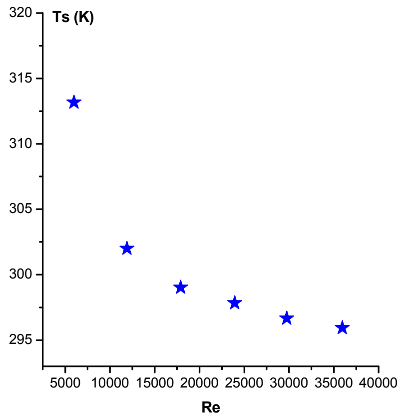

Fig. 9. Outlet temperature Ts versus Reynolds Number

Conclusion

In this paper, we have presented the results obtained by numerical analysis of flow and heat transfer in the air duct of a solar air collector, whose absorber is provided with artificial rectangular ribs. The analysis is based on CFD techniques and was performed using numerical software. This numerical analysis allowed us to found out the effect of absorber roughness on the air flow and heat transfer enhancement in solar air heaters.

The first part of the analysis aims to validate the numerical model by comparing our results to Karwa's experimental results [15]. We have compared between four turbulence closure models and from the results, it is clear that the k-w SST gives the best results.

The second part is an approach to the solar air heater in real operating conditions. This analysis allowed us to visualize the separation and reattachment zones. We also distinguished the over-speed area, where the velocity fluid reaches over 150% its initial velocity.

We have also plotted Nusselt number, hc and Ts evolution with Reynolds number. The global thermohydraulic performance parameter E_T is a good indicator of the effect of artificial ribs in the heat transfer enhancement in solar air heaters. The curve representing its evolution with Reynolds number shows good performance for rectangular ribs used.

Moreover, the geometric shape of roughness studied gave rise to friction factors and therefore not penalizing the thermal-hydraulic performance. So, we recommend the use this type of roughness to improve the thermal performance of solar air collectors.

Acknowledgements

The authors would like to express their gratitude to EMP (Military Polytechnic School) of Algiers, to have allowed us to use their CFD software.

References

[1] Duffie JA, Beckman WA,. Solar engineering of thermal processes. New York: Wiley Interscience publications , NY,1980.
[2] Boulemtafes, A. " Numerical Simulation of Heat Transfer Enhancement in Solar Air heaters", Magister Thesis, USTHB, 2010.
[3] Varun, Saini RP, Singal SK. A review on roughness geometry used in solar air heaters. Solar Energy 2007;81:1340–50.
[4] V. S. Hans, R.P. Saini b, J.S. Saini Performance of artificially roughened solar air heaters—A review, Renewable and Sustainable Energy Reviews 13 (2009) 1854–1869.
[5]. Bhushan B, Ranjit Singh A review on methodology of artificial roughness used in duct of solar air heaters - Energy 35 (2010) 202–212
[6] Lee C.K., S.A. Abdel-moneim Computational analysis of heat transfer in turbulent flow past a horizontal surface with two-dimensional ribs int. Comm. Heat Mass Transfer, 2001,Vol. 28, No. 2. pp. 161-170
[7] Chaube A, Sahoo PK, Solanki SC. Analysis of heat transfer augmentation and flow characteristics of a solar air heater. Renew Energy 2006;31:317–31.
[8] Kumar S., R.P. Saini; CFD based performance analysis of a solar air heater duct provided with artificial roughness, Renewable Energy 34 (2009) 1285–1291. .(article)
[9] Joon Ahn, Joon Sik Lee, Large eddy simulation of flow and heat transfer in a channel with a detached rib array, International Journal of Heat and Mass Transfer 53 (2010) 445–452
[10] Bhatti MS, Shah RK. Turbulent and transition flow convective heat transfer in ducts. Hand book of single-phase convective heat transfer. New York: John Willey & Sons; 1987 [chapter 4].
[11] Joule J.P., On the surface condensation of steam, Philos Trans R Soc Lond, 151, 133-160, 1861.
[12] Nikuradse,J Law of flow in rough pipes. 1950
[13] Webb R.L., Eckert E.R.G. and Goldstein R. J., “Heat transfer and friction in tubes with repeated rib roughness”, International journal of Heat mass transfer, 14, 601-617, 1971.
[14] Lewis M.J., “Optimizing the thermohydraulic performance of rough surfaces”. International journal of Heat mass transfer, 18, 1243-1248, 1975.
[15] Karwa R. Experimental studies of augmented heat transfer and friction in asymmetrically heated rectangular ducts with ribs on heated wall
[16] Gupta D, Solanki SC, Saini JS Heat and fluid flow in rectangular solar air heater ducts having transverse rib roughness on absorber plates. Solar Energy 1993; 51(1): 31-37.
in transverse, inclined, v-continuous and v-discrete pattern. Int Commun Heat Mass Transfer 2003;30:241–50.
[17] Necati Ozisik M. Heat transfer, a basic approach. McGraw-Hill Book Company, 1985.
[18] Tanda G. Heat Transfer in rectangular channels with transverse and V-shaped broken ribs, Int. J. Heat Mass Transfer 47 (2004) 229-243.
[19] Doris L. Introduction à la simulation numérique des écoulements turbulents, cours ENSTA, 2006